Asian Journal of Chemistry; Vol. 23, No. 2 (2011), 847-851

ASIAN JOURNAL OF CHEMISTRY

www.asianjournalofchemistry.co.in

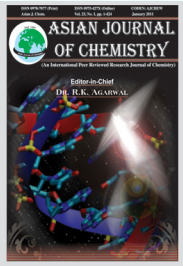

Photocatalytic Degradation of Methylene Blue on Fe-Fullerene/TiO_2 Under Visible-Light Irradiation

ZA-DA MENG[1], KWANG-YOUN CHO[1,2] and WON-CHUN OH[1,*]

[1]Department of Advanced Materials & Science Engineering, Hanseo University, Seosan-si, Chungnam-do 356-706, South Korea
[2]Korea Institute of Ceramic Engineering and Technology, Seoul 1, 153-801, South Korea

*Corresponding author: Fax: +82 41 6883352; Tel: +82 41 6601337; E-mail: wc_oh@hanseo.ac.kr

(*Received*: 26 May 2010; *Accepted*: 12 October 2010) AJC-9180

Three types of Fe-fullerene/TiO_2 were prepared using C_{60} (fullerene) and titanium(IV) *n*-butoxide by a modified sol-gel method. The prepared photocatalysts were characterized by X-ray diffraction, transmission and scanning electron microscopy, energy dispersive X-ray analysis and photocatalytic activity. Photocatalytic properties for decolorization of methylene blue solution in the presence of three types of Fe-fullerene/TiO_2 under visible light had been studied. The results showed that Fe incorporated fullerene enhanced TiO_2 increase the decolorization rate of methylene blue. It was found that the photocatalytic degradation of a methylene blue solution could be attributed to the combined effects caused by the photo-degradation of titania, the electron assistance of fullerene, the enhancement of Fe by photo-fenton effect. The presence of Fe enhanced the photocatalytic actiity of Fe-fullerene/TiO_2 catalysts under visible light.

Key Words: Fe-fullerene/TiO_2, Photocatalytic, Methylene blue, Visible light, TEM.

INTRODUCTION

The material science associated with nano-size carbon materials and the chemistry involved in the preparation of nanocarbon derivatives[1-3], the interesting, higher nano-size carbon materials have received special attention. Recently, carbon-based TiO_2 composites have attracted much attention and have become a very active field of research due to their unique properties and promising applications in pollution management[4,5]. In particular, fullerenes (C_{60}) have attracted considerable attention as of late owing to its remarkable photoelectrical and mechanical properties[6], as well as its subsequent composites that possess intrinsic properties as materials exhibiting cooperative and/or synergetic effects.

Photocatalytic processes are a promising class of advanced oxidation technologies used for environmental remediation[7,8]. Among the photocatalysts, TiO_2 has been intensively investigated for the complete degradation of recalcitrant organic pollutants[8,9], because it is easily available, nontoxic, low-cost and chemically stable. However, TiO_2 has two typical shortcomings to render its wide application in practice: relatively low quantum yield due to the rapid recombination of charge carriers and relatively large bandgap of TiO_2 (3.0 eV for the rutile and 3.2 eV for the anatase phase), it only makes use of the ultraviolet light which contains merely a small portion (*ca.* 3-5 %) of the sunlight's energy.

In order to develop more efficient photocatalyst, various methods have been used to improve the optical properties of TiO_2 by modifying its band gap, such as doping with other elements, sensitizing with dyes, coating the surface with noble metals or other semiconductors[10,11]. Among them, doping is a practical approach because the properties of the material are largely determined by chemical nature of the atoms or ions and of the bonds between them. Through doping with certain metallic or nonmetallic elements, it has been demonstrated that the photo-response of TiO_2 into the visible spectrum by introducing additional energy levels in the band gap of the TiO_2[12-15]. Some metal elements such as Fe, Cu, Mn, Cr and Ni have been employed to tune the electronic structure and enhance the photocatalytic activity of the titanium dioxide[16]. Doping with metal ions may extend the photo-response of TiO_2 into the visible spectrum by introducing additional energy levels in the band gap of the TiO_2. Among these transition metals, Fe, Cu and Mn are able to trap both electrons and holes, while Cr and Ni are capable of trapping only single-charge carriers[17]. The Fe^{3+} ion with the band gap of 2.6 eV seems to be an interesting dopant for extending the absorption threshold toward the visible range[18]. The prepared Fe^{3+} ion doped titania showed a high activity for the photocatalytic under visible light due to the red shift toward the visible range.

The high degree of recombination between photogenerated electrons and holes in semiconductor particles is a

major limiting factor for photodegradation process[19]. Fullerene has attracted extensive attentions for their various interesting properties due to their delocalized conjugated structures and electron-accepting ability. One of the most remarkable properties of fullerene in electron-transfer processes is that it can efficiently arouse a rapid photoinduced charge separation and a relatively slow charge recombination[20]. Thus, the combination of photocatalysts and fullerene may provide an ideal system to achieve an enhanced charge separation by photoinduced electron transfer. Some of the fullerene-donor linked molecules on an electrode exhibited excellent photovoltaic effects upon photo-irradiation[21-23].

In this paper we reported a catalyst based on fullerene, which was prepared by sol-gel process using $Fe(NO_3)_3$ as a dopant to improve the catalytic activity of TiO_2. Characterizations of these catalysts were determined by employing BET, SEM, TEM, XRD and EDX instruments. These catalysts were irradiation with visible light and compare the catalytic activity of this particle with different content of iron.

EXPERIMENTAL

Crystalline fullerene [C_{60}] powder of 99.9 % purity from TCI (Tokyo Kasei Kogyo Co. Ltd., Japan) was used as the carbon matrix. Benzene and ethyl alcohol were purchased as reagent-grade from Duksan Pure Chemical Co. (Korea) and Daejung Chemical Co. (Korea) and used without further purification unless otherwise stated. Ferric nitrate [$Fe(NO_3)_3{\cdot}9H_2O$] as a iron source for the synthesis of the Fe-fullerene compounds was purchased from Duksan Pure Chemical Co. (+ 99 %, ACS reagent, Korea). The titanium(IV) *n*-butoxide (TNB, $C_{16}H_{36}O_4Ti$) as a titanium source for the preparation of the Fe-fullerene/TiO_2 composites was purchased as reagent-grade from Acros Organics (USA). Methylene blue (MB, $C_{16}H_{18}N_3SCl{\cdot}3H_2O$) was analytical grade and also purchased from Duksan Pure Chemical Co., Ltd.

Chemical oxidation on the fullerene surface and Fe treated: *m*-Chloroperbenzoic acid (MCPBA, *ca.* 1 g) was suspended in 50 mL of benzene, followed by the addition of fullerene [C_{60}] (*ca.* 100 mg). The mixture was then refluxed in an air atmosphere and stirred for 6 h. The solvent was subsequently dried at the boiling point of benzene (353.13 K). After completion, the dark brown precipitates were washed with ethyl alcohol and dried at 323 K, after this the oxidation of fullerene was performed. For iron decoration, nomenclatures of samples for the ferric nitrate solution (0.05, 0.10 and 0.50 M) were presented in Table-1. This mixture was refluxed in an air atmosphere and stirred at 343 K for 6 h using a magnetic stirrer in a vial. After being heat treatment at 773 K for 1 h, the Fe-fullerene compounds were formed.

TABLE-1
NOMENCLATURES OF SAMPLES PREPARED WITH FE-FULLERENE/TIO_2 COMPOSITES

Preparation method	Nomenclatures
MCPBA + benzene + C_{60} + 0.05 M $Fe(NO_3)_3$ + TNB	FCT1
MCPBA + benzene + C_{60} + 0.10 M $Fe(NO_3)_3$ + TNB	FCT2
MCPBA + benzene + C_{60} + 0.50 M $Fe(NO_3)_3$ + TNB	FCT3

Preparation of Fe-fullerene/TiO_2 composites: Fe-fullerene was prepared using pristine concentrations of TNB for the preparation of Fe-fullerene/TiO_2 composites. Fe-fullerene powder was mixed with 3 mL of titanium(IV) *n*-butoxide. Then the solutions were homogenized under reflux at 343 K for 5 h, while being stirred in a vial again. After stirred, the solution transformed into Fe-fullerene/TiO_2 gels and these gels were heat treatment at 923 K, then Fe-fullerene/TiO_2 composites were produced.

Characterization of Fe-fullerene/TiO_2 compounds: For the measurements of structural variations, XRD patterns were taken using an X-ray generator (Shimatz XD-D1, Japan) with Cu K_α radiation. SEM was used to observe the surface state and structure of Fe-fullerene/TiO_2 composites using a scanning electron microscope (JSM-5200 Joel, Japan). Energy dispersive X-ray (EDX) was also used for the elemental analysis of the samples. The specific surface area (BET) was determined by N_2 adsorption measurements at 77 K (Monosorb, USA). Transmission electron microscopy (TEM, Jeol, JEM-2010, Japan) were used to observe the surface state and structure of the Fe-fullerene/TiO_2 composites. At acceleration voltage of 200 kV, TEM was used to investigate the size and distribution of the titanium and iron particles deposit on the fullerene surface of various samples. TEM specimens were prepared by placing a few drops of the sample solution on a carbon grid. The whole experimental apparatus were shown in Fig. 1.

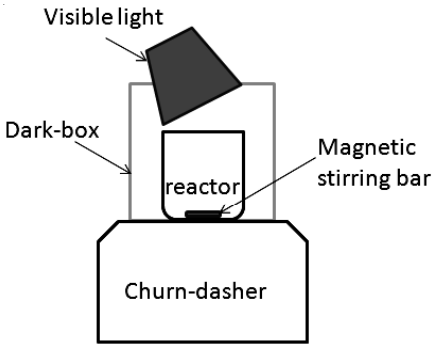

Fig. 1. Schematic illustration of experimental apparatus

Photocatalytic activity measurements: A specified quantity of Fe-fullerene/TiO_2 composites was added to 50 mL methylene blue solution. The reactor was placed for 2 h in the darkness, in order to make the Fe-fullerene/TiO_2 composites particles adsorbed the methylene blue molecule maximum. The initial concentration of the methylene blue was set at 1×10^{-5} mol/L in all experiments. The amount of the Fe-fullerene/TiO_2 composite was 0.05 g/(50 mL solution). After adsorption, photodecomposition of the methylene blue solution was performed under visible light in the dark-box, so that the reactor is irradiated by a single light source. Visible light (35 W LED lamp) irradiation of the photoreactor was done for 10, 30, 60, 90, 120 and 150 min, respectively, to research the degradation of the methylene blue solution. The experiments were performed at room temperature. In the process of degradation of methylene blue, a glass reactor (bottom area = 20 cm^2) was used and the reactor was placed on the magnetic churn dasher. Samples were then withdrawn regularly from the reactor and removal of dispersed powders through a centrifuge. The concentration of methylene blue in the solution was determined as a function of irradiation time.

RESULTS AND DISCUSSION

Structural analysis: The XRD patterns of the samples were prepared with the different amounts of iron are displayed in Fig. 2C is the characteristic peak corresponding to the fullerene, Fig. 2A is anatase phase of titanium, F is Fe and M is Fe_2O_3. It can be seen that the diffraction peaks of all samples are ascribed to the peak of TiO_2 anatase phase to show how much Fe was doped. After heat treatment at 923 K, the major peaks at 25.3, 37.5, 48.0, 53.8, 54.9 and 62.5 were diffractions of (101), (004), (200), (105), (211) and (204) planes of anatase which indicating that the prepared TiO_2 exist in an anatase phase. No peaks for the other TiO_2 phases (rutile or brookite) appear. The results also indicate that the phase transition from titanium(IV) *n*-butoxide to the anatase phase took place at 923 K, with formation of crystalline titania.

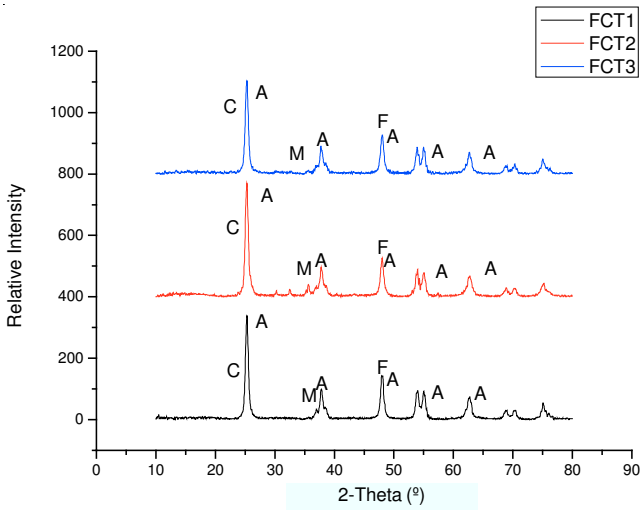

Fig. 2. XRD patterns of Fe-fullerene/TiO_2 composites

The peak of iron is weak because the content of iron is little and the influence of anatase peak. The iron oxides are also shown from this image. The Fe^{3+} ion with the band gap of 2.6 eV seems to be an interesting dopant for extending the absorption threshold toward the visible range. A broad peak is measured at 2θ values of approximately 25.80°. It is the characteristic peak corresponding to the fullerene molecular crystal structure. This peak corresponds to d-values of 0.345 nm[24]. Fullerene and one of titanium characteristic peak are overlap at around 25.0º, so intensity of the peak is increased. Traces of fullerene were detected and a broad diffuse peak in the diffraction pattern is indicative for the presence of amorphous carbon. Moreover, in the curve of samples, we can clearly find the peak of Fe. The characteristic peak of Fe-fullerene in the XRD patterns could not observed. May be iron was in the surface of fullerene, which was further supported by observation *via* SEM, EDX and TEM elemental microanalysis of the Fe-fullerene/TiO_2 composite.

Elemental analysis: Fig. 3 shows the EDX spectra of the prepared photocatalysts compounds. Table-2 listed the results of the EDX elemental microanalysis of the photocatalysts compounds. The EDX data confirms the existence of the main elements, namely C, O, Ti and Fe, as well as other impure elements. The date also shows that most of the spectra for

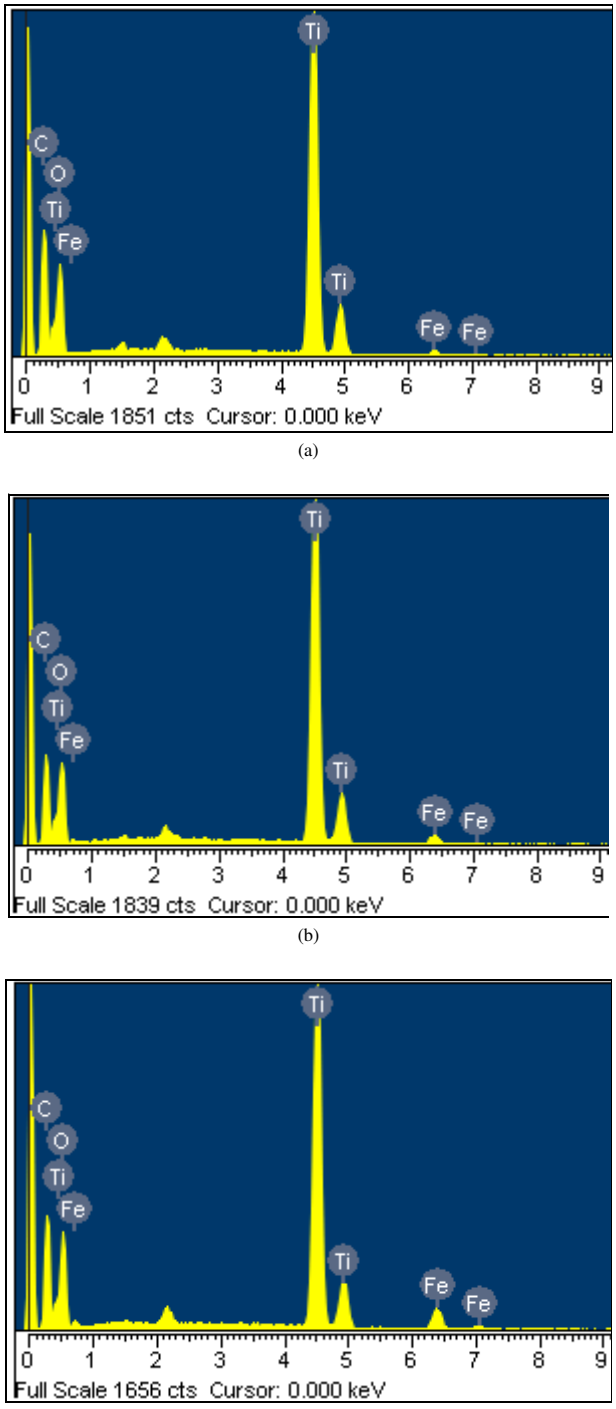

Fig. 3. EDX elemental microanalysis for Fe-fullerene/TiO_2 composite: (a) FCT1, (b) FCT2 and (c) FCT3

TABLE-2
EDX ELEMENTAL MICROANALYSIS OF FE-FULLERENE/TIO_2 COMPOSITES

Sample (wt. %)	C	O	Ti	Fe
FCT1	25.01	40.36	33.73	0.90
FCT2	20.12	41.00	37.08	1.80
FCT3	22.77	40.61	32.08	3.75

these samples produce stronger peaks for carbon and Ti elements than for any other elements. The peak of Fe increased with an enhancement of the dosage of $Fe(NO_3)_3$ during the process of preparation of Fe-fullerene composites. There are

some small impurities which were introduced into the composites using the fullerene without purification. In the case of most of the samples, carbon and titanium were present as major elements with small quantities of oxygen in the composite.

Surface characteristics: The surface characteristics of Fe-fullerene/TiO_2 composites are shown in Fig. 4. SEM micrographs revealed three different Fe-fullerene/TiO_2 composites derivatives with surface characteristics in Fig. 4, it can be clearly seen that the TiO_2 particles prepared at a source temperature of 973 K showed a great distribution of dimension. As shown in Fig. 4, for the Fe-fullerene/TiO_2 composite, the morphological evidences of TiO_2 units onto Fe-fullerene structure which seem to cover on the composite surface. These TiO_2 particles were regularly dispersed on the fullerene surfaces and continuous TiO_2 units were immobilized on almost every grain of fullerene. The large clusters with an irregular agglomerate dispersion could not found, may be the titanium(IV) *n*-butoxide (TNB, $C_{16}H_{36}O_4Ti$) as a titanium source have a low proportion. The crystallite size was also rendered from SEM image. With increased the content of iron, the crystallite size was decreased. With the introduction of iron, the crystallite size is decreased which can be ascribed to the retarding effect of Fe^{3+} on TiO_2 anatase crystallites growth, which favoured the formation of smaller TiO_2 crystallites. It is considered that a good dispersion of small particles on the fullerene surface could provide evidence for the existence of more reactive sites for photodecomposition of the dye[25].

The values of the specific surface area (BET) are shown in Table-3. FCT3 have the largest surface area which can affect the adsorption reaction. The interfacial region of the Fe-fullerene/TiO_2 compound was investigated by TEM to obtain additional information about the interfacial region of the fullerene crystals and to identify potential reaction products in this domain. From Fig. 5, we can see the large cluster with an irregular agglomerate dispersion of TiO_2. The fullerene particles are clearly shown from this picture. The spherical shape is displayed from Fig. 5 which is fullerene. We also found iron element in TEM image, it is revealed as black point.

TABLE-3
SPECIFIC BET SURFACE AREAS OF FE-FULLERENE/TIO_2 COMPOSITES

Sample	S_{BET} (m^2/g)
FCT1	40.4
FCT2	31.3
FCT3	22.5

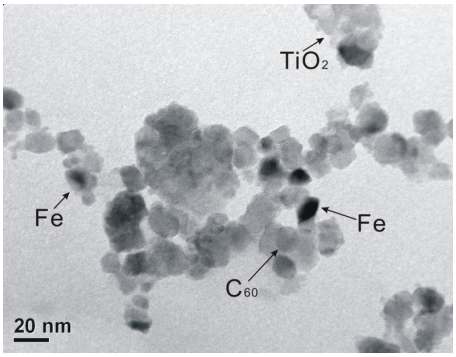

Fig. 5. TEM micrographs of Fe-fullerene/TiO_2 composites

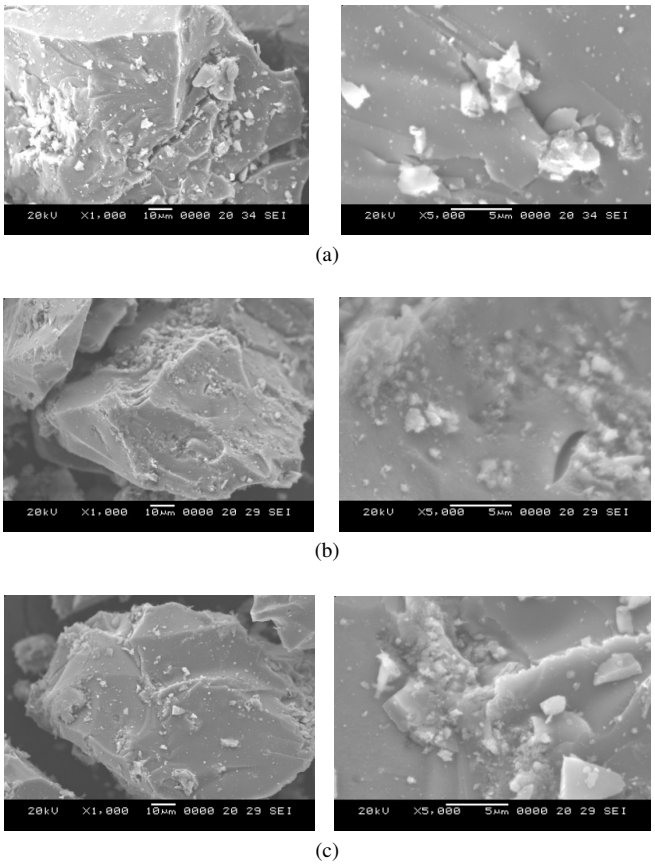

Fig. 4. SEM micrographs of Fe- fullerene/TiO_2 composites: (a) FCT1, (b) FCT2 and (c) FCT3

Photocatalytic decomposition of methylene blue: To study the photocatalytic effect of the prepared samples, we investigated the decomposition reaction of methylene blue in water. The experimental results of the dye removal by the photocatalysts are presented in Fig. 6. The photocatalytic degradation of methylene blue solution under visible light was used for evaluating the photocatalytic activities of different iron content Fe-fullerene/TiO_2 composites. It was found that methylene blue in solution absorbed on FCT1 composites in the dark after 2 h is better than other samples, because of the largest BET numerical value between them. The adsorption

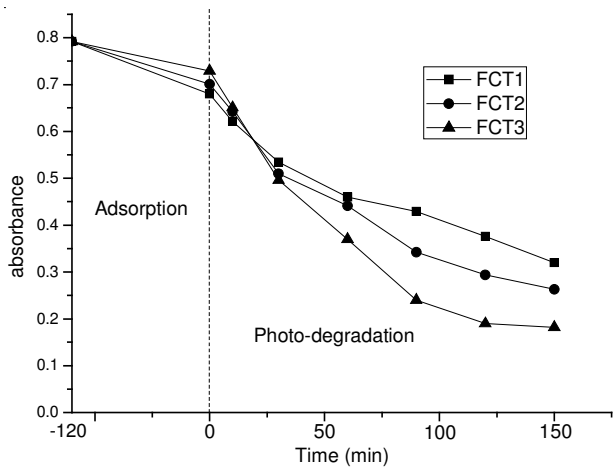

Fig. 6. Effect of the photocatalytic degradation of methylene blue for different Fe-fullerene/TiO_2 composite under visible light

of methylene blue is mainly on fullerene component; fullerene component can improve the compound's adsorption capacity. Fig. 6 shows the absorbance change of organic dye as a function of irradiation time for different samples under visible light. It can be seen that all the Fe-fullerene/TiO_2 composites display higher photocatalytic activity. FCT3 have higher photocatalytic activity compared to FCT1 and FCT2 composites. The data were obtained following a two step experiments. The first step is placed in dark to adsorb dye and the second step is exposed to visible light to degrade methylene blue in solution. From Fig. 6 we can see about 7-14 % of methylene blue molecules were adsorbed in adsorption step, but about 45.9-70.0 % of methylene blue molecules were decomposed in the second step. According to a former study, it is well known that electrons in conduction band and holes valence band are generated on the surface of TiO_2 when it is irradiated with light whose energy equals or exceeds its band gap energy. Theoretically, it is considered that the pure TiO_2 cannot be excited under visible light irradiation because of the lower energy than the band gap. In order to explain the enhanced visible-light-activity of these iron and fullerene doped TiO_2, several possible mechanisms were proposed. As shown in Fig. 7, with the substitution for oxygen atoms by nonmetal atoms (carbon) and Ti^{4+} by Fe^{3+} in the crystal structure of TiO_2, new impurity levels are introduced between the conduction and valence band of TiO_2, then the electrons can be promoted to the conduction band from these impurity levels[26,27]. The electrons can also be promoted from the valence band to another impurity level introduced by iron dopant or from the lower to the higher impurity levels. Therefore, doped Fe-fullerene/TiO_2 photocatalysts have narrower band gap than pure TiO_2 and could increase the absorption in the visible-light region. Subsequently, the departed electrons and holes migrate to the surface of catalysts and react with adsorbed O_2 and H_2O, respectively, forming $O_2^{\cdot-}$ and $OH^{\cdot}$, the main species responsible for the degradation of pollutants, such as methylene blue in our case. With the addition of iron dopant, the reactivity of the catalyst is further increased. There are fewer trapping sites available and Fe^{3+} serves as shallow

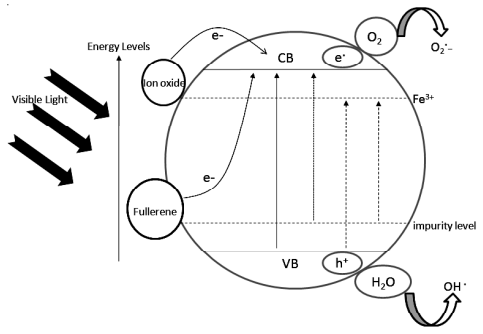

Fig. 7. Schematic diagram of Fe-fullerene/TiO_2 compounds under visible light irradiation

trapping sites for charge carrier (e^- or h^+), thereby separating the arrival time of e^- and h^+ at the surface and increasing the efficiency. The mechanism is also related with doped elemental carbon or carbonaceous species which could act as photosensitizer[28,29]. As shown in Fig. 7, under irradiation of visible-light, the excited photosensitizer injects electrons into the conduction band. The electrons could be further transferred to surface-adsorbed oxygen molecules and form O_2^- and initiates the degradation of methylene blue.

Conclusion

In this study, we presented the fabrication and characterization of Fe-fullerene/TiO_2 composite catalysts. The BET surface area of Fe-fullerene/TiO_2 composites decreased with an increase of Fe component. XRD data revealed that the structure for the Fe-fullerene/TiO_2 composites showed a single anatase crystal phase. The TEM microphotographs of Fe-fullerene/TiO_2 composites showed that fullerene particles were distributed uniformly in the TiO_2 surface and the Fe particles were fixed on the surface of the fullerene, although they were partly aggregated. From the EDX date, the main elements such as C, O, Ti and Fe exited. The FCT3 have higher photo-degradation efficiency than that of other samples. The results demonstrated that the photo-degradation of MB solution could be attributed to synergetic effects of the photo-degradation of TiO_2, the electron assistance of the fullerene, the enhancement of Fe and a function of the applied potential. The morphology of Fe in the Fe-fullerene/TiO_2 composites is an important factor.

REFERENCES

1. W.C. Oh and M.L. Chen, *Bull. Korean Chem. Soc*., **29**, 159 (2008).
2. M.L. Cheng and W.C. Oh, *Carbon Sci*., **8**, 108 (2007).
3. M.R. Hoffmann, S.T. Martin, W. Choi and D.W. Bahnemann, *Chem. Rev*., **95**, 69 (1995).
4. A. Fujishima, T.N. Rao and D.A. Tryk, *J. Photochem. Photobiol. C*., **1**, 1 (2000).
5. K.I. Hadjiivanov and D.K. Klissurski, *Chem. Soc. Rev*., **25**, 61 (1996).
6. A. Heller, *Acc. Chem. Res*., **28**, 503 (1995).
7. J. Wu, S. Hao, J. Lin, M. Huang, Y. Huang, Z. Lan and P. Li, *Cryst. Growth Des*., **8**, 247 (2008).
8. M. Mrowetz, W. Balcerski, A.J. Colussi and M.R. Hoffmann, *J. Phys. Chem. B*, **108**, 17269 (2004).
9. J.C. Yu, J.W Yu, H.Z. Jiang and L. Zhang, *Chem. Mater*., **14**, 3808 (2002).
10. E. Bae and W. Choi, *Environ. Sci. Tech*., **37**, 147 (2003).
11. J.C. Kim, J.K. Choi, Y.B. Lee, J.H. Hong, J.I. Lee, J.W. Yang, W.I. Lee and N.H. Hur, *Chem. Commun*., 5024 (2006).
12. H.G. Kim, D.W. Hwang and J.S. Lee, *J. Am. Chem. Soc*., **12**, 8912 (2004).
13. W.Y. Su, Y.F. Zhang, Z.H. Li, L. Wu, X.X. Wang, J.Q. Li and X.Z. Fu, *Langmuir*, **24**, 3422 (2008).
14. H. Yamashita, M. Harada, J. Misaka, M. Takeuchi, K. Ikeue and M. Anpo, *J. Photochem. Photobiol. A*, **148**, 257 (2002).
15. H. Yamashita, M. Harada, J. Misaka, M. Takeuchi, B. Neppolian and M. Anpo, *Catal. Today*, **84**, 191 (2003).
16. X.B. Chen and S.M. Samuel, *Chem. Rev*., **107**, 2891 (2007).
17. W Choi, A. Termin and M.R. Hoffmann, *J. Phys. Chem*., **98**, 13669 (1994).
18. R.L. Pozzo, M.A. Baltanás and A.E. Cassano, *Catal. Today*, **39**, 219 (1997).
19. A.L. Linsebigler, G. Lu and J.T. Yates Jr., *Chem. Rev*., **95**, 735 (1995).
20. G. Yu, J. Gao, J.C. Hummelen, F. Wudl and A.J. Heeger, *Science*, **270**, 1789 (1995).
21. H. Hotta, S. Kang, T. Umeyama, Y. Matano, K. Yoshida, S. Isoda and H. Imahori, *J. Phys. Chem. B*, **109**, 5700 (2005).
22. D. Hirayama, T. Yamashiro, K. Takimiya, Y. Aso, T. Otsubo, H. Norieda, H. Imahori and Y. Sakata, *Chem. Lett*., 570 (2000).
23. D.F. Liu, S.H. Yang and S.-T. Lee, *J. Phys. Chem. C*, **112**, 7110 (2008).
24. W.C. Oh, A.R. Jung and W.B. Ko, *Mater. Sci. Eng. :C*, **29**, 1338 (2009).
25. A. Smontara, A. M. Tonejc, S. Gradecak, A. Tonejc, A. Bilusicand and J.C. Lasjaunias, *Mster. Sci. Em.: C*., **19**, 21 (2002).
26. F.A. Khalid, O. Beffort, U. E. Klotz, B. A. Keller, P. Gasser and S. Vaucher, *Acta. Mater*., **51**, 4575 (2003).
27. Z.N. Gu, L. Zhang, J.L. Margrave, V.A. Davydov, A.V. Rakhmanina, V. Agafonov and V.N. Khabashesku, *Carbon*, **43**, 2989 (2005).
28. X. Yang, C. Cao, K. Hohn, L. Erickson, R. Maghirang and K. Klabunde, *J. Catal*., **252**, 296 (2007).
29. X. Yang, C. Cao, L. Erickson, K. Hohn, R. Maghirang and K. Klabunde, *J. Catal*., **260**, 128 (2008).